

134. Sykes, M. Hematopoietic cell transplantation for tolerance induction: animal models to clinical trials. *Transplantation* **87**, 309–316 (2009).
135. Kode, J. A., Mukherjee, S., Joglekar, M. V. & Hardikar, A. A. Mesenchymal stem cells: immunobiology and role in immunomodulation and tissue regeneration. *Cytotherapy* **11**, 377–391 (2009).
136. de, V. M., Crouch, B. G., van, P. L. & van, B. D. Pathologic changes in irradiated monkeys treated with bone marrow. *J. Natl Cancer Inst.* **27**, 67–97 (1961).
137. Lochte, H. L. Jr, Levy, A. S., Guenther, D. M., Thomas, E. D. & Ferrebee, J. W. Prevention of delayed foreign marrow reaction in lethally irradiated mice by early administration of methotrexate. *Nature* **196**, 1110–1111 (1962).
138. Epstein, R. B., Storb, R., Ragde, H. & Thomas, E. D. Cytotoxic typing antisera for marrow grafting in littermate dogs. *Transplantation* **6**, 45–58 (1968).
139. Storb, R., Rudolph, R. H. & Thomas, E. D. Marrow grafts between canine siblings matched by serotyping and mixed leukocyte culture. *J. Clin. Invest.* **50**, 1272–1275 (1971).
140. Bach, F. H., Albertini, R. J., Joo, P., Anderson, J. L. & Bortin, M. M. Bone-marrow transplantation in a patient with the Wiskott-Aldrich syndrome. *Lancet* **2**, 1364–1366 (1968).
141. Gatti, R. A., Meuwissen, H. J., Allen, H. D., Hong, R. & Good, R. A. Immunological reconstitution of sex-linked lymphopenic immunological deficiency. *Lancet* **2**, 1366–1369 (1968).
142. O'Reilly, R. J. *et al.* Reconstitution in severe combined immunodeficiency by transplantation of marrow from an unrelated donor. *N. Engl. J. Med.* **297**, 1311–1318 (1977).
143. Hansen, J. A. *et al.* Transplantation of marrow from an unrelated donor to a patient with acute leukemia. *N. Engl. J. Med.* **303**, 565–567 (1980).
144. Deeg, H. J. *et al.* Cyclosporin A and methotrexate in canine marrow transplantation: engraftment, graft-versus-host disease, and induction of intolerance. *Transplantation* **34**, 30–35 (1982).
145. Reisner, Y. *et al.* Transplantation for acute leukaemia with HLA-A and B nonidentical parental marrow cells fractionated with soybean agglutinin and sheep red blood cells. *Lancet* **2**, 327–331 (1981).
146. Reisner, Y. *et al.* Transplantation for severe combined immunodeficiency with HLA-A, B, D, DR incompatible parental marrow cells fractionated by soybean agglutinin and sheep red blood cells. *Blood* **61**, 341–348 (1983).
147. Spangrude, G. J., Heimfeld, S. & Weissman, I. L. Purification and characterization of mouse hematopoietic stem cells. *Science* **241**, 58–62 (1988).
148. Kolb, H. J. *et al.* Donor leukocyte transfusions for treatment of recurrent chronic myelogenous leukemia in marrow transplant patients. *Blood* **76**, 2462–2465 (1990).
149. Slavina, S. *et al.* Allogeneic cell therapy: the treatment of choice for all hematologic malignancies relapsing post BMT. *Blood* **87**, 4011–4013 (1996).
150. Raju, T. N. The Nobel chronicles. 1990: Joseph Edward Murray (b 1919) and E Donnall Thomas (b 1920). *Lancet* **355**, 1282 (2000).

#### Acknowledgements

The authors would like to acknowledge T. Pederson, V. He, M. Pasquini and M. Horwitz for the Center for International Blood and Marrow Transplant Research survival data presented, as well as M. Perales, J. Barker and J. Jurcic for critical comments on the manuscript.

#### Competing interests statement

The authors declare no competing financial interests.

#### DATABASES

Entrez Gene: <http://www.ncbi.nlm.nih.gov/gene>  
 ECRL3 | MTHFR | NOD2 | TLR4 | TLR4 | TNE | TRA | TRB  
 National Cancer Institute Drug Dictionary: <http://www.cancer.gov/drugdictionary>  
 plerixafor  
 UniProtKB: <http://www.uniprot.org>  
 ABL | BCR | CD34 | CXCL12 | CXCR4 | GCSF | IL-2 | IL-7 | IL-15 | IL-21 | PR3 | TERT | WT1

#### FURTHER INFORMATION

Marcel R. M. van den Brink's homepage:  
<http://www.mskcc.org/mskcc/html/10937.cfm>  
 ALL LINKS ARE ACTIVE IN THE ONLINE PDF

## TIMELINE

# Dissecting cancer through mathematics: from the cell to the animal model

Helen M. Byrne

**Abstract** | This Timeline article charts progress in mathematical modelling of cancer over the past 50 years, highlighting the different theoretical approaches that have been used to dissect the disease and the insights that have arisen. Although most of this research was conducted with little involvement from experimentalists or clinicians, there are signs that the tide is turning and that increasing numbers of those involved in cancer research and mathematical modellers are recognizing that by working together they might more rapidly advance our understanding of cancer and improve its treatment.

That mathematical modelling has an integral role in the resolution of engineering and physics problems that impinge on our daily life is undisputed. By contrast, the role of mathematics in generating mechanistic insight into biological problems, including the development and growth of solid tumours, is less well known. This probably reflects either a lack of collaboration with experimentalists, or perhaps that the mathematical models have been unintelligible to most biomedical researchers! The main aim of this Timeline article is to redress this imbalance by celebrating the major achievements that have been made through combining mathematical models with biological models of cancer and to show how cross-disciplinary collaboration can accelerate progress in understanding and treating this disease (TIMELINE). With limited space we must be selective, therefore, this article focuses on mathematical models of carcinogenesis, avascular and vascular tumour growth and angiogenesis to best illustrate this process.

#### Application of mathematical models

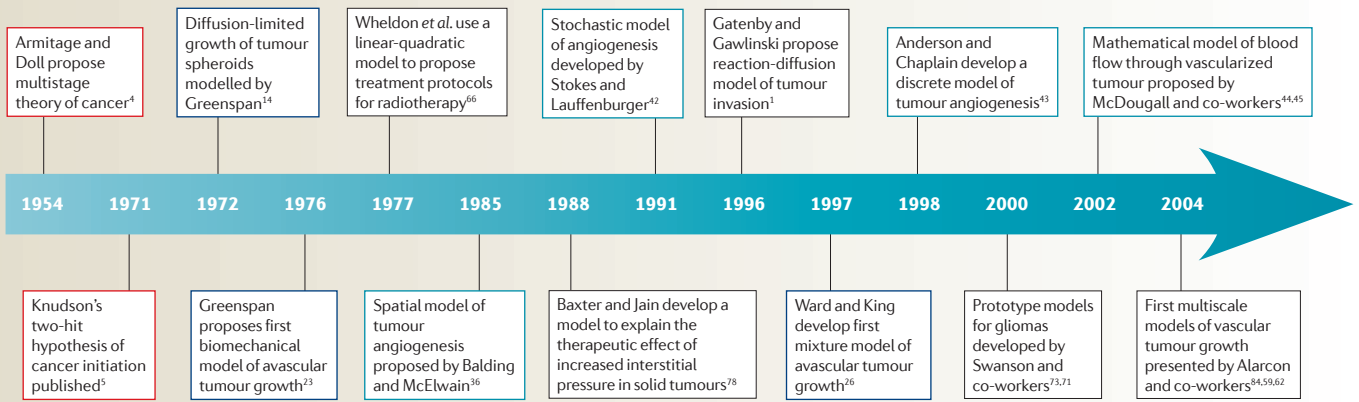
When applied to experimental data, statistical techniques can reveal whether a particular intervention produces a significant response or whether a correlation exists between observable phenomena. Establishing why such correlations arise requires the statement of hypotheses postulating which physical processes are involved and how they interact. The biological experiments needed to test such hypotheses can be time-consuming, expensive and/or impossible with existing technology. In such cases, mathematical

modelling can have an intermediate role, by providing an independent check of the consistency of the hypotheses: if a model is unable to reproduce the observed phenomena, then the original hypotheses should be revised before continuing. Mathematical models can also improve experimental design by highlighting which measurements are needed to test a particular theory and whether additional information can be gained by collecting supplementary data.

These ideas are summarized in FIG. 1, which also provides a guide to the stages involved in model building. Mathematical modelling is an iterative process that should not end with the first set of predictions and its success relies on continued collaboration between experimentalists and theoreticians. An excellent illustration of the benefits of such interactions is provided by a mathematical model developed by Gatenby and Gawlinski<sup>1</sup> to test the acid-mediated invasion hypothesis for tumour spread. The model predicted that under certain circumstances a gap would arise between the advancing tumour front and the regressing normal tissue, a prediction that was subsequently verified experimentally.

When challenged by sceptics who question whether mathematical models of cancer will ever be used as predictive tools, we should take heart from the cardiac models developed by Noble, Hunter and colleagues<sup>2</sup> that have secured approval from the US Food and Drug Administration for drug testing. With such models for inspiration, the construction of similar ones for cancer becomes a more attainable, albeit challenging, vision for the future.

Timeline | History of mathematical modelling of cancer



The differently coloured boxes denote models of the same type: red for models of carcinogenesis; dark blue for models of avascular tumour growth; light blue for models of angiogenesis.

**Carcinogenesis and cancer incidence**

Armitage and Doll's multistage theory<sup>3</sup> is one of the earliest models of cancer initiation and was motivated by the analysis of cancer mortality statistics<sup>4</sup>. The theory states that the age distribution of a cancer will increase with a power of age that is one less than the number of changes (not necessarily mutations) needed for its progression<sup>3</sup>. Therefore, the incidence rate  $I(t)$  of cancer at age  $t$  is

$$I(t) = kt^n \tag{1}$$

where  $n$  is the number of stages through which a cell must pass before becoming malignant and  $k$  is a constant of proportionality. Therefore, seven cellular changes are necessary for cancers with incidence rates that increase with the sixth power of age. Although Armitage and Doll's theory provides an excellent description of cancers of the colon, stomach and pancreas, it fails to describe the incidence of others, including breast and prostate cancer. Additionally, it provides no mechanistic insight into the functional changes responsible for disease progression.

By analysing similar incidence data for retinoblastoma, Knudson<sup>5</sup> proposed that only two 'hits' or changes are needed to cause the disease: children with familial retinoblastoma are born with the first hit, increasing their chances of acquiring the second hit and explaining why they present with retinoblastoma earlier than those with sporadic disease. The identification of the *RBI* tumour suppressor gene in 1987 confirmed Knudson's two-hit hypothesis. This theory of loss of tumour suppression has helped to characterize the inactivation of other tumour suppressor genes such as adenomatous polyposis coli (*APC*) in colon

cancer and *TP53*, which is mutated in more than 50% of human tumours.

Although providing excellent descriptions of cancer incidence data, these models and their extensions are unable to link the data with the functional changes associated with tumour progression. Newer models, based on Hanahan and Weinberg's 'Hallmarks of cancer' (REF. 6), are now being used to investigate how the sequence and timing of mutations and the environmental conditions influence tumour progression<sup>7-9</sup>. Others<sup>10</sup> are developing models of somatic evolution or studying the effect of chromosomal instability and microsatellite instability on tumour initiation<sup>11,12</sup>. For example, Komarova *et al.*<sup>11</sup> used optimal control theory to identify, from a set of physically realistic, time-varying mutation rates (or controls), the mutation rate that enables a population of cancer cells to most rapidly attain a given size. Their analysis showed that, for most choices of parameter values, the optimal strategy for the tumour could be characterized by a mutation rate that is initially high and reduces over time. This prediction is consistent with the behaviour of many cancers that show a high degree of genetic instability during early growth and stabilize as the disease progresses. By exploiting increases in computing power and the availability of large data sets, Siegmund *et al.*<sup>12</sup> have recently applied statistical methods to DNA methylation patterns to infer the genetic evolution of colorectal cancer cells at several sites in the tumour. As the ancestral trees from different sites revealed a common ancestor at the time of transformation, they went on to conclude that the cancers were probably initiated by a period of rapid clonal expansion, rather than being established at different times by different cells.

**Avascular tumour growth**

The earliest spatio-temporal models of avascular tumour growth<sup>13,14</sup> describe how the size and structure of three-dimensional multicellular spheroids (MCS) change when culture conditions are manipulated<sup>15</sup>. The simplicity and reproducibility of the experimental assays for MCS, the availability of reliable data on the size and composition of the spheroids and information about the spatial distributions of key metabolites (such as oxygen and glucose) and chemotherapeutic drugs, made MCS attractive subjects for mathematical modelling. It is also likely that, during their discussions with biologists, these pioneering mathematicians were further motivated when they realized that analogous models had already been developed to describe a range of physical systems, including the expansion of metals in response to heat and the freezing of liquids. In each case the size of the material of interest (tumour, metal or solid) changes over time and its growth rate is regulated by the transport of a diffusible species (oxygen or glucose for the tumour, temperature change for the metal and liquid) through the material.

Today, these early models of MCS can seem extremely simple, and perhaps even naive, particularly in comparison to the detailed computational models that are currently being developed to study solid tumour growth (discussed below). For example, the spheroids are assumed to be radially symmetric and their growth regulated by a single, diffusible growth factor that is supplied externally (such as oxygen) or produced internally (such as tumour necrosis factor). The distribution of a growth factor in the spheroid regulates its local dynamics, with expansion when cell growth exceeds death

and regression otherwise. By integrating these contributions over the tumour volume we arrive at the following equation, which relates the time evolution of the tumour radius  $R(t)$  to  $c(r,t)$ , the distribution of growth factor in the spheroid:

$$\frac{dR}{dt} = \frac{1}{R^2} \int_{r=0}^R F(c)r^2 dr \quad (2)$$

In this equation, the function  $F(c)$  models the influence of the growth factor  $c$  on the net cell growth rate at each point in the spheroid. For example, if  $c$  represents oxygen or glucose then we can assume that  $F$  increases as  $c$  increases, and that it approaches a maximum value for large values of  $c$ . The spatial distribution of  $c$  is determined by solving a diffusion equation in the form:

$$\frac{\partial c}{\partial t} = \frac{D}{r^2} \frac{\partial}{\partial r} \left( r^2 \frac{\partial c}{\partial r} \right) - g(c,R) \quad (3)$$

where  $D$  represents the diffusion coefficient of  $c$ , and  $g(c,R)$  describes its local rate of consumption. As for  $F(c)$ , this function is growth factor-specific and might depend on whether the cells are proliferating, quiescent or dying. The distribution of the growth factor can also be used to predict spheroid structure. For example, threshold values of oxygen can delineate regions of cell proliferation (high oxygen), quiescence (intermediate oxygen) and necrosis (low oxygen) (FIG. 2). Models of the above form show excellent qualitative and quantitative agreement with experimental data on MCS (FIG. 2). Typically, an initial exponential growth phase is superseded by a transient, linear phase during which the width of the outer proliferating rim remains constant, until eventually the tumour reaches an equilibrium size at which the net rates of cell growth and death balance. Analytic expressions for the size of the spheroid at the onset of quiescence and the width of its outer, proliferating rim during the linear growth phase can be used to estimate model parameters and predict the effect of changing the concentration of the key growth factor being supplied to the spheroid<sup>16</sup>. The agreement between the experimental data on MCS and the dynamics of the mathematical models indicates that the models provide a realistic description of the biological processes that regulate the growth of MCS. Such agreement does not constitute a 'proof' that these mechanisms alone regulate the MCS. Other models, based on different assumptions, may show equally good agreement with these data. We illustrate this point in FIG. 2, where we present results obtained from using a continuum model developed by Owen and co-workers<sup>17</sup> and results from an alternative,

discrete, cell-based model from Jiang and co-workers<sup>18</sup>.

In such situations, in which different theoretical approaches seem to be equally compatible with the experimental data, it can be difficult to decide which approach is the better one. In practice, this depends on the questions that the model is being used to address and the type of data available. In general, cell-based models can be more easily extended to account for additional data on subcellular signalling pathways and/or the cell cycle, whereas continuum models contain fewer parameters and, as a result, should give better fits to the data. Additionally, if simulations from the different approaches yield qualitatively different behaviour (such as their predicted response of an MCS to exposure to a particular drug), then these can be used to design experiments that will discriminate between the two types of models.

Owing to their simplicity, the early models of MCS have limited applicability. For example, the spheroids are assumed to comprise a single population of cells, and stochastic effects are ignored, so that the emergence of different clonal subpopulations can not be investigated. Equally, cell metabolism is assumed to be controlled by a single diffusible species, whereas in practice multiple metabolites are involved. In particular, as tumour cells become starved of oxygen they switch from aerobic to anaerobic respiration.

The extensions and modifications to Greenspan's original model of MCS are now so numerous that it is impossible to do justice to them here (for details see REFS 19–22). Important developments include relaxing the assumption of radially symmetric growth<sup>23–25</sup> and distinguishing different cell populations within the spheroid<sup>26</sup>. For example, whereas Greenspan<sup>23</sup> used analytical techniques to predict how the invasive boundary of a tumour initially develops, Cristini and colleagues<sup>25</sup> used sophisticated numerical methods to solve the system of nonlinear equations and relate the irregular shapes adopted by the tumour to the values of key model parameters. They predicted that highly vascularized tumours would remain compact in shape while they grew, whereas those with limited nutrient availability would develop invasive fingers, leading to tumour fragmentation.

Although the initial focus of MCS models was on diffusible growth factors, the introduction of cell movement and pressure marked a conceptual change to accommodate mechanical effects. For example, in the model presented by Greenspan in 1976 (REF. 23) pressure gradients, generated by differences in cell proliferation and death, cause cells to move from regions of high cell proliferation and pressure (near the tumour periphery) to regions of net cell death and lower pressure (at the tumour

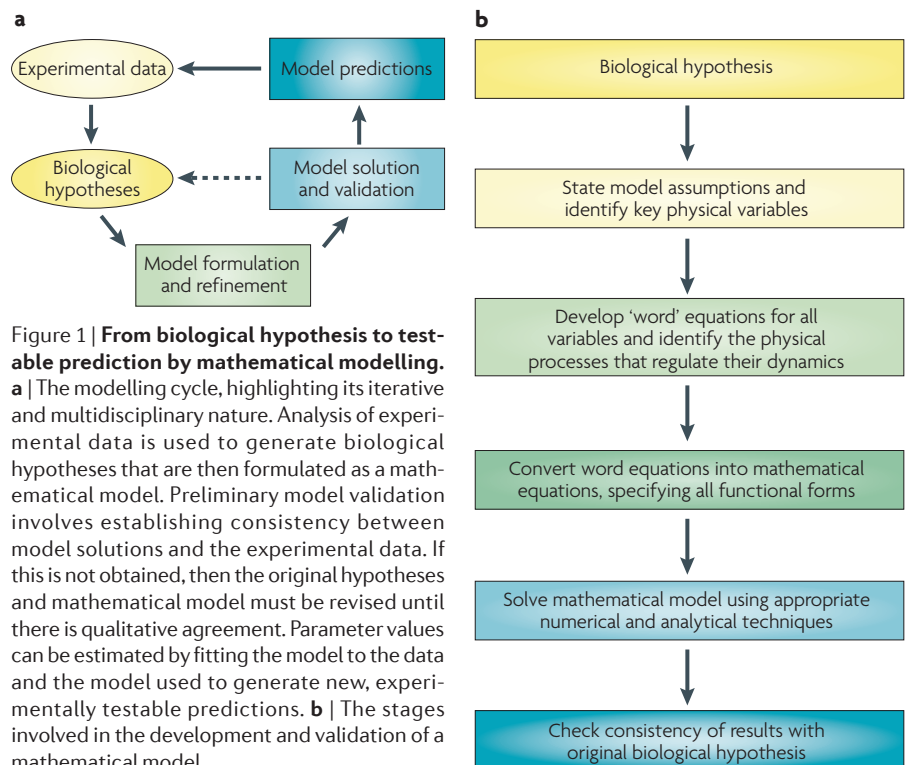


**Figure 1 | From biological hypothesis to testable prediction by mathematical modelling.** **a** | The modelling cycle, highlighting its iterative and multidisciplinary nature. Analysis of experimental data is used to generate biological hypotheses that are then formulated as a mathematical model. Preliminary model validation involves establishing consistency between model solutions and the experimental data. If this is not obtained, then the original hypotheses and mathematical model must be revised until there is qualitative agreement. Parameter values can be estimated by fitting the model to the data and the model used to generate new, experimentally testable predictions. **b** | The stages involved in the development and validation of a mathematical model.



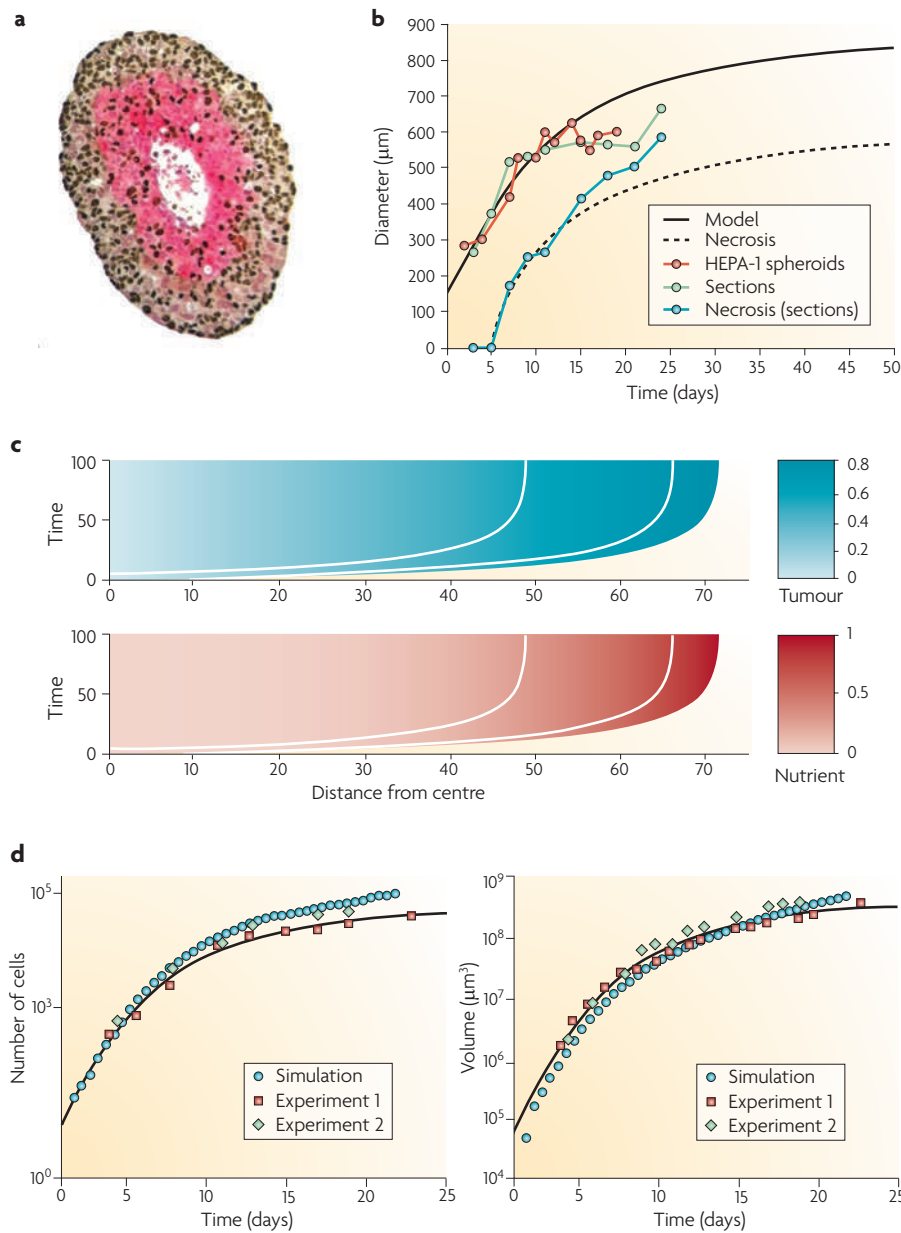


**Figure 2 | Alternative approaches for modelling the growth of multicellular spheroids (MCS).** **a** | A cross-section through a mature human breast cancer spheroid (diameter 800  $\mu\text{m}$ ). The nuclei of proliferating cells are stained brown (bromodeoxyuridine labelling) and the hypoxic cells are stained red (pimonidazole staining). The hypoxic cells surround a central necrotic core, and the proliferating cells are concentrated in the outer, well-oxygenated areas of the spheroid. Photograph courtesy of C. E. Lewis, University of Sheffield, UK. **b** | The continuum model provides a good fit to experimental data for the growth of HEPA-1 spheroids<sup>18</sup>. The solid line represents the position of the outer tumour boundary and the dashed line the position of the necrotic boundary. Reproduced, with permission, from REF. 17 © (2004) Elsevier. **c** | These graphs were generated from a continuum model of MCS growth<sup>18</sup>. They show how the distribution of tumour cells and a nutrient (oxygen in this example) in an MCS change over time as the MCS grows to equilibrium. At equilibrium, the rate at which nutrient-rich cells near the boundary proliferate balances the rate at which nutrient-starved cells near the centre die. The solid white lines are contours of the nutrient concentration that mark the transitions from cell proliferation to hypoxia (outer curve) and from hypoxia and necrosis (left-most curve). Reproduced, with permission, from REF. 17 © (2004) Elsevier. **d** | These graphs illustrate how similar results can be obtained by fitting a multiscale model of MCS growth to data from EMT6/Ro spheroids grown in culture medium containing 0.08 mM oxygen and 5.5 mM glucose<sup>18</sup>. They show how the number of cells and the spheroid volume change over time. The squares represent experimental data, the circles represent simulation results and the solid lines are the best fit assuming Gompertzian growth. Reproduced, with permission, from REF 18 © (2005) Elsevier.

centre). Additionally, either surface tension or cell–cell adhesion is assumed to maintain the compact nature of the tumour mass and counter the expansive forces that are associated with tumour growth. Routine model analysis reveals that the strength of cell–cell adhesion — the affinity of the cells to remain as a coherent mass — strongly influences spheroid morphology: strong cell–cell adhesion yields radially symmetric spheroids, and weak adhesion yields irregular, fractal-like spheroid boundaries. This suggests that mutations that weaken cell–cell adhesion might be a characteristic feature of highly invasive tumours.

Other authors have developed biomechanical models in which the tumour is seen as a mixture of interacting phases, for example cells and extracellular fluid cultured in suspension<sup>26,27</sup> or embedded in a tissue matrix. Several independent models<sup>28–30</sup> have shown that the growth-induced compression of a compliant tissue matrix (or gel) that surrounds a tumour spheroid can generate restraining forces that arrest the growth of the spheroid, even when nutrients are freely available. Further, stiffer tissues give rise to smaller spheroids. These results suggest that knowledge of the mechanical properties of a tumour and its surrounding tissue might be important for characterizing invasive potential. They also explain how therapies designed to alter the mechanical properties of the tissue stroma by, for example, neutralizing the action of matrix-degrading proteases, might retard invasion. In practice, the tissue stroma surrounding a tumour is heterogeneous and subject to continuous remodelling<sup>31,32</sup>. New mathematical models that link stromal remodelling and tumour growth are needed to explain how processes such as collagen deposition, cross-linking and degradation by stromal fibroblasts contribute to tumour growth and how they could be manipulated for therapeutic advantage.

Models such as those presented above are continuum models because they describe how cell populations and concentrations change and, in contrast to discrete cell-based models, they do not distinguish between individual cells. Therefore, continuum models share several common features: the tumours are seen as continuous masses that contain a small number of distinct populations, stochastic effects are usually neglected and subcellular phenomena are ignored. As such, they are well suited to studying the growth kinetics of tumour spheroids that contain a large number of cells but less well suited to small clusters of tumour cells, such as metastases. For studying small spheroids,

discrete models (such as cellular automata) that view the tumour as a collection of interacting cells, each assigned their own set of parameter values and behavioural rules, are gaining in popularity and have been used to study tumour invasion<sup>33</sup> and the emergence and fixation of clonal subpopulations<sup>7,8</sup>. For example, in a series of papers, Anderson and co-workers<sup>8,33</sup> have used cellular automata to investigate how the microenvironment (specifically, the local oxygen concentration and extracellular matrix density) influences (and is influenced by) the growth dynamics and phenotypic diversity of a tumour<sup>8,33</sup>. Their simulations predicted that when oxygen levels are low the tumour will rapidly diverge from its initial phenotype and exhibit high levels of population diversity, with aggressive phenotypes quickly becoming dominant.

When comparing cell-based and continuum models of tumour growth, an obvious advantage of cell-based models is the relative ease with which parameters to model their behaviour can be chosen using measurable biological and biophysical quantities, such as cell growth rates during the cell cycle and cell membrane deformation in response to mechanical loading. Given that tumours growing *in vitro* and *in vivo* typically contain between  $10^6$  and  $10^{11}$  cells, it might be more practical to use a continuum rather than a cell-based model to simulate their development. In recent work, Byrne and Drasdo<sup>34</sup> have developed complementary cell-based and continuum models of MCS growth that exhibited similar growth kinetics. By fitting the profiles for the tumour radius and pressure distribution generated by each model they estimated parameters for the continuum model from parameters in the cell-based model. In this way, they have shown how cell-based models can be used as an intermediate step to relate measurable biophysical properties of individual cells to parameters that appear in continuum models of MCS. More recently, Kim and co-workers<sup>35</sup> have developed a new type of hybrid model in which a continuum model is used in regions with a high tumour cell density and a discrete model is used in regions with a tumour cell density that is too low to justify the use of a continuum model.

### Tumour angiogenesis

In 1985, Balding and McElwain<sup>36</sup> proposed a simple model of tumour angiogenesis to describe experiments in which tumour cells implanted in the rabbit cornea stimulated the formation, growth and migration of new blood vessels from the limbus to

the tumour<sup>37</sup>. The model focuses on a generic, tumour-derived chemical, termed a tumour angiogenesis factor (TAF), as well as capillary tips and vessels that we denote by  $a$ ,  $n$  and  $b$ , respectively. The model is set up so that TAF that is produced by the tumour cells diffuses towards neighbouring vessels and also undergoes natural decay. For a one-dimensional model, with  $x$  representing the distance from the vasculature to the tumour centre, these assumptions supply the following equation for  $a(x,t)$ :

$$\frac{\partial a}{\partial t} = D_a \frac{\partial^2 a}{\partial x^2} - \mu_a a \quad (4)$$

where  $D_a$  denotes the assumed constant diffusion coefficient of the TAF and  $\mu_a$  its natural decay rate. In addition, the tumour is assumed to produce TAF at a constant rate so that the concentration of TAF at the tumour boundary (for example,  $x = L$ ) is maintained at a constant value,  $a_c$ . The capillary tips are assumed to emanate from existing vessels and tips at rates that increase with increasing TAF levels, to move by chemotaxis up spatial gradients of TAF and to form tip-to-tip anastomosis. Combining these effects we obtain the following equations for  $n(x,t)$ :

$$\frac{\partial n}{\partial t} = -\chi \frac{\partial}{\partial x} \left( n \frac{\partial a}{\partial x} \right) + (\lambda_{nb} b + \lambda_{nn} n) \left( \frac{a}{\kappa_\partial + a} \right) - \mu_n n - v_n n^2 \quad (5)$$

In this equation,  $\chi$  is the chemotaxis coefficient,  $\lambda_{nb}$  and  $\lambda_{nn}$  are the rates at which tips emerge from existing vessels and tips,  $\mu_n$  is the net rate at which capillary tips die and  $v_n$  is the rate at which they form tip-to-tip anastomoses. As they migrate towards the tumour, the capillary tips extend behind them a 'snail trail' of new vessels. Under these assumptions the equation for the vessels  $b(x,t)$  reads:

$$\frac{\partial b}{\partial t} = \chi_n \frac{\partial a}{\partial x} - \mu_b b \quad (6)$$

where  $\mu_b$  represents the rate at which vessels regress or die.

Numerical simulations of Balding and McElwain's model and its subsequent extensions<sup>38</sup> reproduce many characteristic features of angiogenesis, including acceleration of the developing vasculature towards the tumour implant and a peak in the density of capillary tips preceding a peak in the density of blood vessels<sup>39</sup>. The models have also been used to compare anti-angiogenic therapies that neutralize TAF with others that block endothelial cell chemotaxis or inhibit endothelial cell proliferation<sup>38</sup>. These effects

can be investigated by altering the relevant model parameter. For example, a reduction in the chemotaxis coefficient  $\chi$  would mimic the effect of a therapy that blocks endothelial cell chemotaxis. Alternatively (and more realistically), an additional reaction diffusion equation, similar to that for the TAF  $a(x,t)$ , can be introduced to describe the drug of interest and the relevant model parameters modified to account for its mode of action. The basic models have also been extended to account for tumour growth during angiogenesis and the increase in nutrient availability associated with the expanding vasculature<sup>40</sup>.

Extensions of the early models of tumour angiogenesis to two and three spatial dimensions highlight their main weaknesses<sup>41</sup>. For example, as the vessels are treated as a single model variable, only variations in their concentration are considered and details of the morphology of the vascular network are ignored. Consequently, such models are unable to distinguish between a tissue perfused by one large vessel and another perfused by a large number of small vessels, even though the amount of oxygen being delivered to the two tissues might vary markedly. Vascular remodelling and the effect of blood flow on the evolving vasculature are also neglected. These deficiencies have stimulated the development of a new class of hybrid models that account for the detailed morphology of the angiogenic network. Hybrid models combine two or more different modelling approaches. For example, reaction-diffusion equations for nutrient transport and consumption can be coupled to a cellular automaton that describes how normal and tumour cells interact. Stokes and Lauffenburger<sup>42</sup> coupled a probabilistic equation for the movement of individual endothelial cells to a diffusion equation for TAF. Their simulations revealed that a chemotactic response to a TAF is necessary for stimulating directed vascular network growth and that a substantial level of random motion is required for vessel anastomosis and capillary loop formation — an overly strong chemotactic response produced networks largely devoid of these features. By obtaining independent qualitative and quantitative agreement of their model with *in vitro* and *in vivo* experiments, they not only demonstrated that *in vitro* migration assays can be used to test putative inhibitors and activators of angiogenesis but also highlighted an important role of mathematical modelling as a bridge between *in vitro* and *in vivo* experiments.

More recently, Chaplain and co-workers<sup>43</sup> have developed a hybrid model in which

capillary tip movement is treated as a random walk, which is biased towards higher levels of TAF and blood flow is included<sup>44</sup>. In addition to simulating angiogenic networks that resemble those seen *in vivo*, these models can also be used to predict the distribution of blood-borne chemotherapeutic agents<sup>45</sup>.

As more information about the underlying biochemistry has become available, more detailed mathematical models have been developed. For example, Levine *et al.*<sup>46,47</sup> proposed a model to account for specific pro-angiogenic and anti-angiogenic factors (such as vascular endothelial growth factor A (VEGFA)), angiopoietin 1 (ANGPT1), ANGPT2, anti-angiogenic compounds (such as endostatin and angiostatin) and protease inhibitors, and interactions between the endothelial cells that line the blood vessels and other cell types (such as between pericytes and macrophages). More recently, Bentley *et al.*<sup>48</sup> have developed an agent-based model to investigate how crosstalk between neighbouring endothelial cells might regulate angiogenic sprouting: a feedback loop is assumed to link delta-like 4–Notch-mediated lateral inhibition to changes in the number of VEGF receptors expressed by a particular cell<sup>48</sup>. Model simulations have generated several predictions — for example, a spatial gradient in VEGF is postulated to increase the rate of tip selection — and these are now being tested in the laboratory.

Additionally, large and complex mathematical models of key signalling pathways and regulatory networks are increasingly being used to study angiogenesis<sup>49,50</sup>. Wu *et al.*<sup>51</sup> used a compartmental model to show that a naturally occurring and soluble form of VEGF receptor 1 (VEGFR1) does not significantly inhibit VEGF signalling and concluded that any observed inhibitory effects might be due to heterogeneity in blood flow. Although such models provide valuable, state-of-the-art descriptions of biological knowledge, it might be difficult to obtain reliable estimates of every parameter and to disentangle which processes are responsible for observed behaviours. In such situations, a series of increasingly detailed models of the same pathway might be needed and decisions made about which model to use based on the question of interest, the type of data that can be collected and, therefore, the number of system parameters that can be reliably estimated. Important challenges associated with this approach include establishing how different models of the same pathway are related, whether parameters in one model can be estimated from measurements of parameters in another and predicting how different pathways interact. These challenges arise because the alternative models are based on different physical assumptions: a process that is neglected in one model might be retained in another. Equally, different functions, with different numbers of parameters, can be used to describe the same biological process.

**Vascular tumour growth**

In contrast to avascular tumours, which can be easily studied in the laboratory and have highly reproducible growth patterns, vascular tumours must be grown *in vivo* and their growth dynamics are extremely diverse. Indeed, owing to the interplay between the rapidly proliferating tumour cells and the evolving vasculature, the composition of a single tumour can be highly heterogeneous in both space and time. For example, a functioning blood vessel can, over time, become occluded or collapse owing to the pressure exerted on it by the increasing number of tumour cells that it supports. The associated reduction in nutrient supply could stimulate the tumour cells to produce angiogenic factors that will regulate the growth of new blood vessels into the region<sup>37,52,53</sup>. These factors, combined with the technical challenge of collecting information about how the spatial composition of a vascular tumour changes over time, have frustrated mathematicians attempting to model vascular tumour growth. As a result, until recently, only a small number of mathematical models of vascular tumour growth had been proposed.

In 1999, Hahnfeldt *et al.*<sup>54</sup> proposed a simple model, formulated as a system of differential equations, coupling the growth of the tumour mass and its vasculature: the maximum tumour burden was assumed to be proportional to the vascular volume and the tumour cells could stimulate the formation of new vessels through angiogenesis.

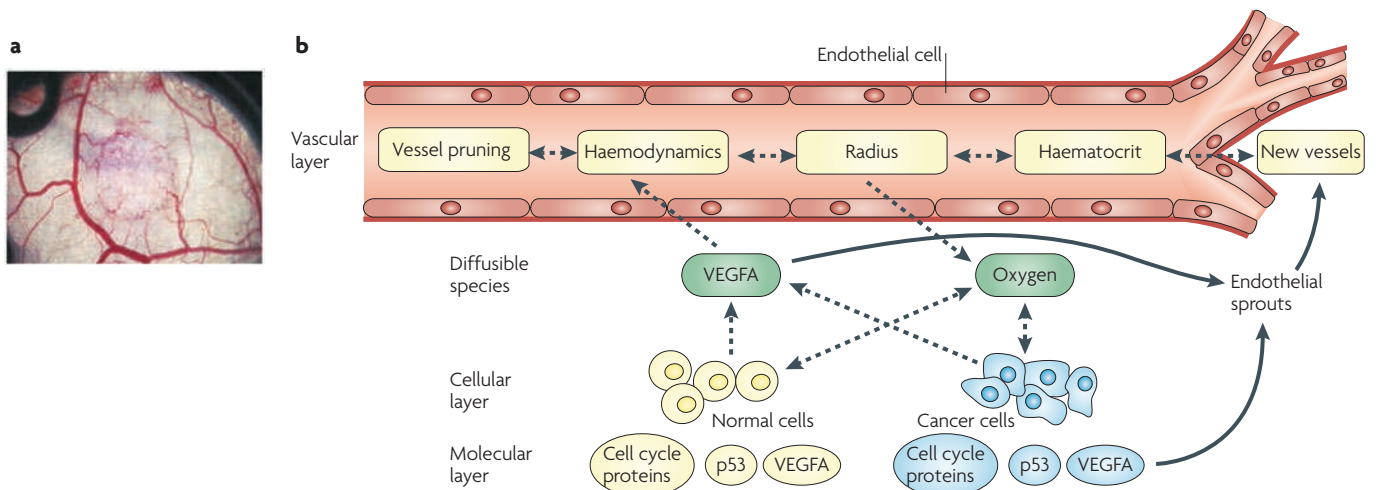


**Figure 3 | Multi-scale modelling of vascular tumour growth. a** | An intravital microscopy image of a human colorectal carcinoma (HT29) that has been growing for 7 days in a dorsal skin fold window chamber in an immunocompromized male mouse. Vascularization of the tumour is shown (mean diameter: 1.7 mm). Photograph courtesy of G. M. Tozer, University of Sheffield, UK. **b** | Representation of a multi-scale model that integrates processes acting on different time and size scales<sup>62</sup>. Phenomena at the tissue scale include blood flow, structural adaptation

of the vascular network and transport of diffusible species such as oxygen and vascular endothelial growth factor (VEGF); at the cellular level, competition between cancer and normal cells and the release of growth factors such as VEGF are implemented in simple rules for a cellular automaton. At the subcellular level ordinary differential equations model progress through the cell cycle, apoptosis and the production of key proteins, such as VEGF and p53. Reproduced, with permission, from REF. 62 © (2009) Springer.



After fitting their model to experimental data in which anti-angiogenic agents were administered to mice with Lewis lung tumours they used it to predict that treatment with a combination of specific doses of angiostatin and endostatin would yield a linear, additive response — a prediction that was verified in further *in vivo* experiments. Similar models, involving systems of differential equations, have been developed to investigate the contributions of angiogenesis and vasculogenesis to the growth and treatment of vascular tumours<sup>55,56</sup>. More detailed models that also account for the influence of VEGF and the angiopoietins on vessel maturation have been used to show how the strength of the angiogenic response affects the growth rate of a tumour<sup>57</sup>. In particular, low vessel maturation rates in tumours with low background vessel densities will give rise to slowly growing tumours that possess large proportions of immature vessels and might exhibit oscillatory growth dynamics<sup>57</sup>.

Following the model published by McDougall *et al.*<sup>44</sup>, similar hybrid models of vascular tumour growth have been developed to investigate interactions between a tumour and its vasculature. For example, by coupling a cellular automaton model with a system of reaction-diffusion equations for key metabolites, Patel and co-workers<sup>58</sup> studied the effect of vascular density and tumour metabolism on the invasive potential of tumour cells that could survive at lower pH levels than normal cells. The vasculature was assumed to be non-adaptive and modelled as a series of localized sources (sinks) of glucose ( $H^+$  ions, which are representative of pH levels). Numerical simulations revealed a range of vascular densities for which tumour growth and invasion were optimal: at lower densities, excessively low pH levels cause both normal and tumour cells to die and at higher densities the vessel network rapidly eliminates any acid that is produced, so it is maintained at low levels and the tumour cells lose their competitive advantage over normal cells.

In practice, the tumour vasculature is a highly dynamic network, with new vessels being produced to meet the metabolic demands of under-perfused, hypoxic tumour regions while redundant vessels, with low flow, are pruned at other sites. Various multi-scale models are now being developed to account for these and other features<sup>44,59–63</sup>. For example, Macklin and colleagues<sup>63</sup> have shown that the inclusion of extracellular matrix degradation by tumour cells can hinder newly formed blood vessels from penetrating the tumour mass. This results in the generation of vascular

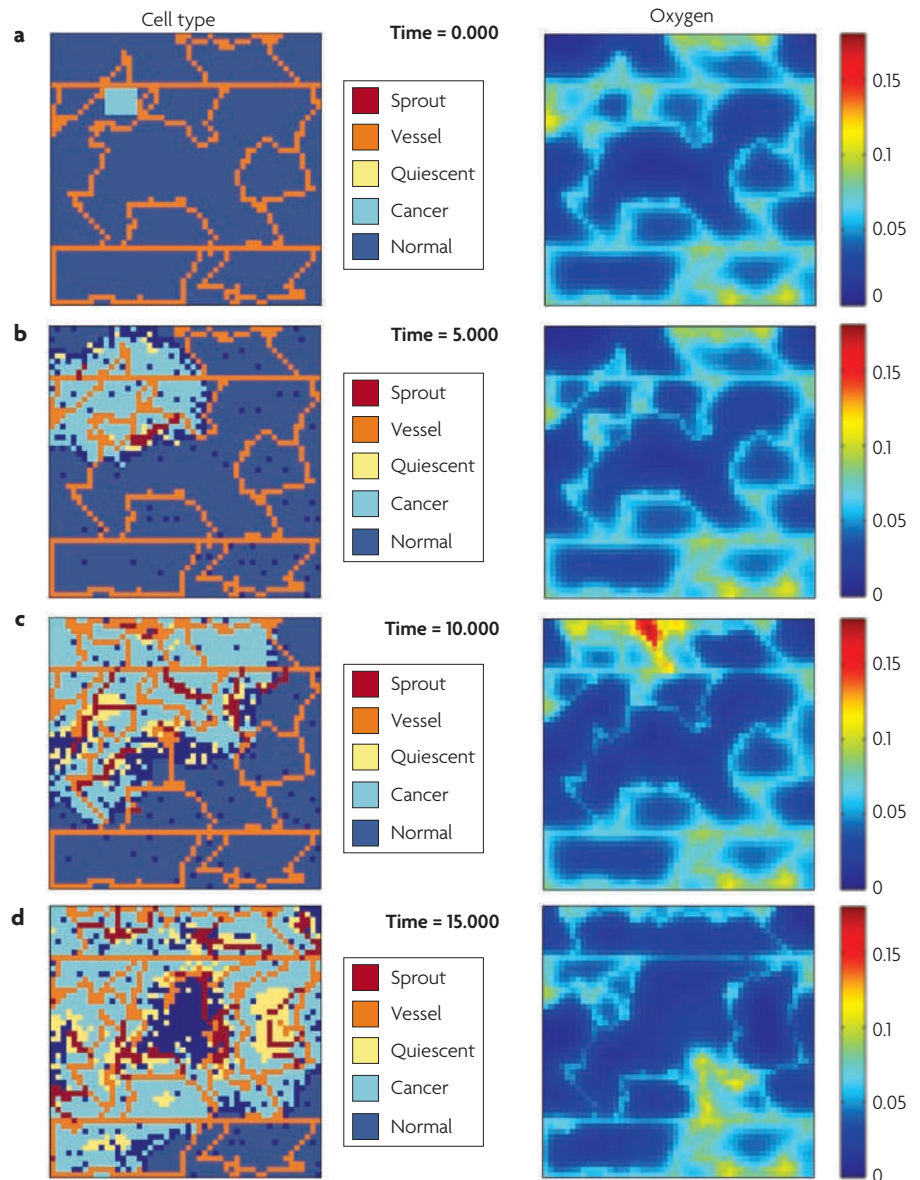


**Figure 4 | A mathematical model of vascularized tumour growth.** These images show the results from a typical multi-scale simulation of the growth of a tumour seeded in a vascularized tissue (FIG. 3). Initially, the tumour expands preferentially in the direction of the blood vessels, where oxygen levels are high. Excessive proliferation leads to the appearance of transient regions of hypoxia, which are sources of vascular endothelial growth factor (VEGF) and stimulate the in-growth of new blood vessels. Movies of these simulations are found in [Supplementary information S1–4](#) (movies).

networks that encapsulate the tumour mass and are inefficient at delivering nutrients to the tumour. Alarcón and co-workers<sup>59</sup> have developed a computational framework that couples processes that function at the sub-cellular, cellular and tissue scales<sup>62</sup> (FIGS 3–5). Although these models are complex, they can be used to investigate the importance of feedback between processes that operate at different spatial scales. For example, if blood flow is assumed to be uniform in the vasculature then the tumour grows as a compact mass, whereas if it is heterogeneous, with the flow in each vessel varying as the network

evolves, then the pattern of tumour growth is highly irregular<sup>59</sup>. The models also support the emerging concept that treatment with anti-angiogenic compounds can transiently normalize the structure and function of the tumour vasculature and therefore reduce the degree of tumour hypoxia and enhance the response to chemotherapy<sup>64</sup>.

#### Mathematical models in the clinic

In addition to being a powerful tool for dissecting out the mechanisms that regulate solid tumour growth, mathematical modelling can contribute to the rational design

of optimal treatment protocols involving combinations of surgery, chemotherapy and radiotherapy and the development of new therapies<sup>65</sup>. For example, the linear-quadratic law, an empirical formula relating the proportion of cells that survive exposure to a dose of ionizing radiation, forms the basis of many radiotherapy protocols. By extending the linear-quadratic model to account for exponential regrowth of the tumour between treatments and using elementary calculus, Wheldon and co-workers<sup>66</sup> derived expressions for the number of rounds of therapy, the interval between treatments and the radiation dose that should be applied to maximize tumour cell kill while ensuring that the damage to healthy tissue does not exceed a threshold value. Other groups have extended the linear-quadratic model to account for the effects of hypoxia<sup>67</sup>, more complex growth laws<sup>68</sup> and cellular heterogeneity<sup>69</sup>. A common weakness of these models is that the tumour is treated as a spatially uniform mass. Accordingly, Swanson and co-workers have recently incorporated the linear-quadratic model into a spatio-temporal, reaction-diffusion model of glioma growth and invasion to compare the efficacy of different schedules and radiation dose distributions<sup>70</sup>. In earlier work, Swanson and co-workers<sup>71</sup> applied their reaction-diffusion model to magnetic resonance imaging (MRI) data from patients with glioma to simulate glioma regrowth following surgery. They used this model to predict the time to relapse and to determine whether chemotherapy can significantly extend time to relapse<sup>71</sup>.

A related area in which mathematical modelling could have an important future role is the integration of images acquired using different modalities. For example, Swanson and colleagues<sup>72</sup> reported a strong correlation between the invasiveness and degree of hypoxia of gliomas, their estimates of invasiveness being obtained from MRI data<sup>73</sup> and their estimates of hypoxia from 18 F-fluoromisonidazole-positron emission tomography (PET) images. New mathematical models that link hypoxia and invasion could be used, in conjunction with PET and MRI data, to establish a mechanistic basis for the observed correlation and, in the longer term, to guide treatment concepts.

The co-registration of images collected for diagnosis and/or under different conditions is a related area in which mathematics could have a valuable role. Consider, for example, X-ray images and MRI taken before surgery for breast cancer. During X-ray mammography the patient stands

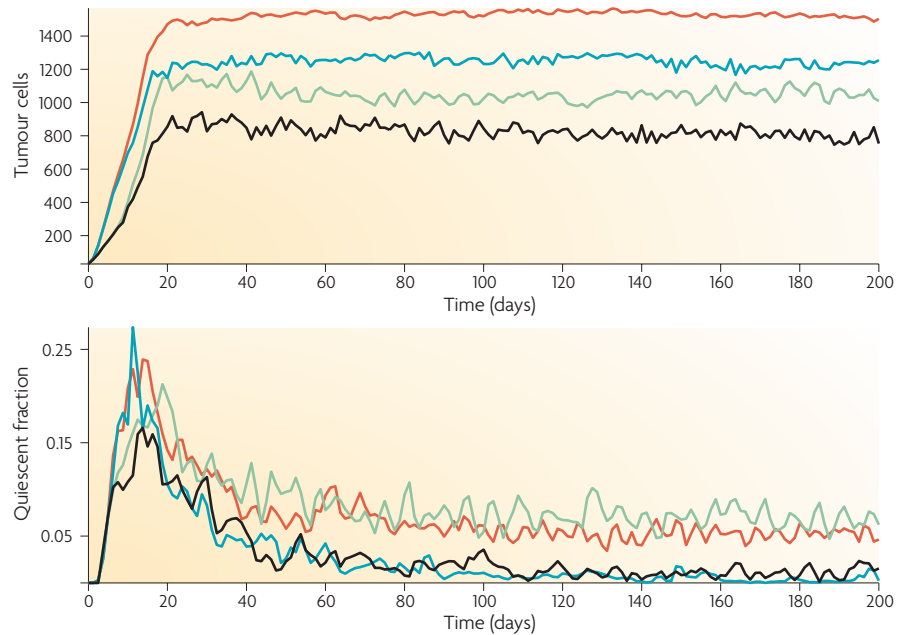


**Figure 5 | Changes in tumour cell growth after drug exposure.** The graphs show how tumour cell number and proportion of the tumour that is hypoxic change on exposure to conventional chemotherapy or a specific immunotherapy. The immunotherapy used in this experiment involves genetically engineered macrophages that, when localized in hypoxic tumour regions, release an enzyme that activates a pro-drug. If present at sufficiently high levels, the activated drug kills tumour cells when they divide. For each treatment strategy, numerical results were obtained by introducing chemotherapy and immunotherapy into a multi-scale model of vascular tumour growth (FIGS 3,4) and spatially averaging the data from ten simulations. The numerical results indicate that chemotherapy used in isolation (green line) effects a greater reduction in tumour burden than the immunotherapy (blue line), although the proportion of quiescent cells is higher. Combined treatment (black line) gives the greatest reduction in tumour size. The red line represents the growth of the untreated tumour cells. Movies of these simulations are found in Supplementary information S1–4 (movies).

and the breast is compressed between plates by up to 60%; during MRI mammography the patient is prone and the breast hangs freely. Nonlinear elasticity combined with knowledge of the mechanical properties of normal and diseased breast tissue can be used to estimate, from the X-ray image, the shape the breast will take when the patient is prone<sup>74</sup> so that more accurate co-registration of the X-ray and MRI data can be achieved. Such information might, in the longer term, be used to predict the shape of the breast when the patient is undergoing surgery thereby providing precise guidance on the location and size of tissue to be excised.

As discussed above, mathematical models can also be used to determine the mode of action of new compounds<sup>75–77</sup> (FIG. 5) and to identify new targets for drug design<sup>49,51</sup>. For example, Wu *et al.*<sup>51</sup> have developed a multi-scale, compartmental model of the body that models the transport of two isoforms of VEGFA (VEGF<sub>121</sub> and VEGF<sub>165</sub>) and their interaction with VEGFR1, VEGFR2 and the non-signalling co-receptor neuropilin 1, as well as how

these interactions are altered by the presence of soluble VEGFR1 (sVEGFR1), which can function as a ligand trap but has also been shown to interact with VEGF receptors. Model simulations designed to determine what processes are responsible for the observed anti-angiogenic activity of sVEGFR1 have revealed that VEGF sequestration by sVEGFR1 can not produce a significant anti-angiogenic effect in isolation. The authors conclude that the interaction of sVEGFR1 with VEGFR1 in addition to sequestration of the ligand is probably needed to affect VEGFA levels.

Using a simpler, stochastic model of VEGFA signalling in endothelial cells, Alarcón and Page<sup>49</sup> showed that tumour-mediated overexpression of VEGFRs in endothelial cells of tumour vessels increases their sensitivity to low levels of VEGF and thereby endows the tumour with increased resistance to anti-angiogenic treatments. These results also suggest that compounds that target the processes responsible for VEGFR overexpression on endothelial cells might prevent tumours becoming resistant to anti-angiogenic agents.



In earlier work, Jain and co-workers<sup>78</sup> developed continuum models to identify likely causes for poor drug delivery to vascular tumours. Their models revealed that although irregular blood flow and perfusion hinder drug delivery to vascular tumours, increased interstitial fluid pressure has a more substantial role, by driving fluid radially outwards from the tumour and opposing the extravasation of the drugs. These predictions have been confirmed by experiments and are stimulating the development of new treatments that can overcome these barriers to drug delivery<sup>17</sup>.

### Conclusions

Confronted with the vast array of mathematical approaches being used to study tumour growth<sup>19–22,79,80</sup>, it can be difficult to decide what type of model is best suited to a particular problem and what level of detail to include. The situation can be further exacerbated when we realize that different mathematical approaches can reproduce the same experimental results (FIG. 2)! In such cases, it may be appropriate to appeal to Occam's razor to develop a model that includes sufficient detail to address the question of interest but not so much that it becomes obscured in detail. In practice, close collaboration between theoreticians and biomedical researchers is crucial to getting this balance right, because the models are only ever as good as the assumptions used to construct them and the data with which they are validated. Indeed, in many respects the form of the initial model is less important than starting the dialogue between experimentalists and modellers because the model is almost certain to be wrong. In the same way that a new experimental protocol requires testing and optimization before data collection can begin, the mathematical model will require refinement before it can be applied to a real problem. To date, most of the mathematical modelling that has been carried out has been retrospective, being developed in response to a set of experimental data or to test a biological hypothesis. If theoreticians play a more pro-active part in the design of experimental programmes then the models that they develop should complement the experimental data, and vice versa. Additionally, the quality and practical use of the mathematical models should also increase and contribute to improved treatment and a better prognosis for cancer patients worldwide.

Looking to the future, as technological advances enable more accurate and high-throughput measurement of physical

quantities, our reliance on mathematics is likely to further increase, not least because mathematical models, particularly multi-scale ones, are natural frameworks for combining the different types of data that will be collected. For example, multi-scale models have the potential to establish how changes in protein and gene expression at the sub-cellular level influence (and are influenced by) processes, such as invasion and vascular adaptation, which occur at the tissue scale.

In conclusion, mathematical models represent a natural framework for not only testing biological hypotheses and generating new ones but also optimizing experimental protocols. As we survey the large body of research devoted to modelling tumour growth, it is clear that considerable progress has been made (TIMELINE), although its full effect has yet to be realized. Therefore, many of the tools (or models) have been developed: what is now needed are people who can translate these prototypes into validated models that are specialized for particular tumours and drugs, with the power to generate both qualitative and quantitative predictions. The increasing number of modelling papers appearing in the literature<sup>81–83</sup> indicates that this transition is starting to happen.

Helen M. Byrne is at the Centre for Mathematical Medicine and Biology, School of Mathematical Sciences, University of Nottingham, Nottingham NG7 2RD, UK.  
e-mail: Helen.byrne@nottingham.ac.uk

doi:10.1038/nrc2808

- Gatenby, R. A. & Gawlinski, E. T. A reaction-diffusion model of cancer invasion. *Cancer Res.* **56**, 5745–5753 (1996).
- Noble, D. Computational models of the heart and their use in assessing the actions of drugs. *J. Pharmacol. Sci.* **107**, 107–117 (2008).
- Nordling, C. O. A new theory on the cancer-inducing mechanism. *Br. J. Cancer* **7**, 68–72 (1953).
- Armitage, P. & Doll, R. The age distribution of cancer and multistage theory of carcinogenesis. *Br. J. Cancer* **8**, 1–12 (1954).
- Knudson, A. G. Mutation and cancer: statistical study of retinoblastoma. *Proc. Natl Acad. Sci. USA* **68**, 820–823 (1971).
- Hanahan, D. & Weinberg, R. The hallmarks of cancer. *Cell* **100**, 57–70 (2000).
- Spencer, S. L., Gerety, R. A., Pienta, K. J. & Forrest, S. Modelling somatic evolution in tumorigenesis. *PLoS Comput. Biol.* **2** e108 (2006).
- Quaranta, V., Rejniak, K. A., Gerlee, P. & Anderson, A. R. Invasion emerges from cancer cell adaptation to competitive microenvironments: quantitative predictions from multiscale mathematical models. *Semin. Cancer Biol.* **18**, 338–348 (2008).
- Smallbone, K., Gavanagh, D. J., Gatenby, R. A. & Maini, P. K. The role of acidity in solid tumour growth and invasion. *J. Theor. Biol.* **235**, 476–484 (2007).
- Nowak, M. A., Michor, F. & Iwasa, Y. The linear process of somatic evolution. *Proc. Natl Acad. Sci. USA* **100**, 14966–14969 (2003).
- Komarova, N. L., Sadovsky, A. V. & Wan, F. Y. M. Selective pressures for and against genetic instability in cancer: a time-dependent problem. *J. Roy. Soc. Interface* **5**, 105–121 (2008).
- Siegmund, K. D., Marjoram, P., Woo, Y. J., Tavaré, S. & Shibata, D. Inferring clonal expansion and cancer stem cell dynamics from DNA methylation patterns in colorectal cancers. *Proc. Natl Acad. Sci. USA* **106**, 4828–4833 (2009).
- Burton, A. C. Rate of growth of solid tumours as a problem of diffusion. *Growth* **30**, 157–176 (1966).
- Greenspan, H. P. Models for the growth of a solid tumour by diffusion. *Stud. Appl. Math.* **52**, 317–340 (1972).
- Folkman, J. & Hochberg, M. Self-regulation of growth in three-dimensions. *J. Exp. Med.* **138** 745–753 (1973).
- Byrne, H. M. & Chaplain, M. A. J. Necrosis and apoptosis: distinct cell loss mechanisms? *J. Theor. Med.* **1**, 223–236 (1998).
- Owen, M. R., Byrne, H. M. & Lewis, C. E. Mathematical modelling of the use of macrophages as vehicles for drug delivery to hypoxic tumour sites. *J. Theor. Biol.* **226**, 377–391 (2004).
- Jiang, Y., Pjesivac-Grbovic, Cantrell, C. & Freyer, J. P. A multiscale model for avascular tumour growth. *Biophys. J.* **89**, 3884–3894 (2005).
- Araujo, R. P. & McElwain, D. L. S. A history of the study of solid tumor growth: the contribution of mathematical modelling. *Bull. Math. Biol.* **66**, 1039–1091 (2004).
- Preziosi, L. *Cancer modelling and simulation*. (CRC, Boca Raton, USA, 2003).
- Tracqui, P. Biophysical models of tumor growth. *Rep. Prog. Phys.* **72**, 29 Apr 2009 (doi:10.1088/0034-4885/72/5/056701).
- Roose, T., Chapman, S. J. & Maini, P. K. Mathematical models of avascular tumour growth: a review. *SIAM Rev.* **49**, 179–208 (2007).
- Greenspan, H. P. On the growth and stability of cell cultures and solid tumours. *J. Theor. Biol.* **56**, 229–242 (1976).
- Byrne, H. M. & Chaplain, M. A. J. Modelling the role of cell-cell adhesion in the growth and development of carcinomas. *Math. Comput. Model.* **24**, 1–17 (1996).
- Cristini, V., Lowengrub, J. & Nie, Q. Nonlinear simulation of tumor growth. *J. Math. Biol.* **46**, 191–224 (2003).
- Ward, J. P. & King, J. R. Mathematical modelling of avascular tumour growth. *IMA J.* **14**, 39–69 (1997).
- Byrne, H. M., King, J. R., McElwain, D. L. S. & Preziosi, L. A two-phase model of solid tumour growth. *Appl. Math. Lett.* **16**, 567–573 (2003).
- Helmlinger, G., Netti, P. A., Lichtenbeld, H. C., Melder, R. J. & Jain, R. K. Solid stress inhibits the growth of multicellular tumour spheroids. *Nature Biotech.* **15**, 778–783 (1997).
- Chen, C. Y., Byrne, H. M. & King, J. R. The influence of growth-induced stress from the surrounding medium on the development of multicell spheroids. *J. Math. Biol.* **43**, 191–220 (2001).
- Roose, T., Netti, P. A., Munn, L. L., Boucher, Y. & Jain, R. K. Solid stress generated by spheroid growth estimated using a linear poroelasticity model. *Microvasc. Res.* **66**, 204–212 (2003).
- Radisky, D. C., Kenny, P. A. & Bissell, M. J. Fibrosis and cancer: do myofibroblasts come also from epithelial cells via EMT? *J. Cell Biochem.* **101**, 830–839 (2007).
- Bertheim, U., Hofer, P. A., Engström-Laurent, A. & Hellström, S. The stromal reaction in basal cell carcinomas. A prerequisite for tumour progression and treatment strategy. *Br. J. Plast. Surg.* **57**, 429–439 (2004).
- Anderson, A. R. A hybrid mathematical model of solid tumour invasion: the importance of cell adhesion. *Math. Med. Biol.* **22**, 163–186 (2005).
- Byrne, H. & Drasdo, D. Individual-based and continuum models of growing cell populations: a comparison. *J. Math. Biol.* **58**, 657–687 (2009).
- Kim, Y., Stolarska, M. A. & Othmer, H. G. A hybrid model for tumor spheroid growth *in vitro* I: Theoretical development and early results. *Math. Model. Meth. Appl. Sci.* **17** S1773–S1798 (2007).
- Balding, D. & McElwain, D. L. S. A mathematical model of tumour-induced capillary growth. *J. Theor. Biol.* **114**, 53–73 (1985).
- Folkman, J., Tumour angiogenesis. *Adv. Cancer Res.* **19**, 331–358 (1974).
- Byrne, H. M. & Chaplain, M. A. J. Mathematical models for tumour angiogenesis: numerical simulations and nonlinear wave solutions. *Bull. Math. Biol.* **57**, 461–486 (1995).
- Muthukaruppan, V. R., Kubai, L. & Auerbach, R. Tumour-induced neovascularisation in the mouse eye. *J. Natl. Cancer Inst.* **69**, 699–705 (1982).
- Panovska, J., Byrne, H. M. & Maini, P. K. A theoretical study of the response of vascular tumours to different types of chemotherapy. *Math. Comput. Model.* **47**, 560–579 (2008).

41. Orme, M. E. & Chaplain, M. A. Two-dimensional models of tumour angiogenesis and anti-angiogenesis strategies. *IMA J.* **14**, 189–205 (1997).
42. Stokes, C. L. & Lauffenburger, D. A. Analysis of the roles of microvessel endothelial cell random motility and chemotaxis in angiogenesis. *J. Theor. Biol.* **152**, 377–403 (1991).
43. Anderson, A. R. A. & Chaplain, M. A. J. Continuous and discrete mathematical models of tumour-induced angiogenesis. *Bull. Math. Biol.* **60**, 857–899 (1998).
44. McDougall, S. R., Anderson, A. R., Chaplain, M. A. & Sherratt, J. A. Mathematical modelling of flow through vascular networks: implications for tumour-induced angiogenesis and chemotherapy strategies. *Bull. Math. Biol.* **64**, 673–702 (2002).
45. McDougall, S. R., Anderson, A. R. & Chaplain, M. A. Mathematical modelling of dynamic adaptive tumour-induced angiogenesis: clinical implications and therapeutic targeting strategies. *J. Theor. Biol.* **241**, 564–589 (2006).
46. Levine, H. A., Sleeman, B. D. & Nilsen-Hamilton, M. A mathematical model for the roles of pericytes and macrophages in the initiation of angiogenesis. I. The role of protease inhibitors in preventing angiogenesis. *Math. Biosci.* **168**, 77–115 (2000).
47. Levine, H. A., Tucker, A. L. & Nilsen-Hamilton, M. A mathematical model for the role of cell signal transduction in the initiation and the inhibition of angiogenesis. *Growth Factors* **20**, 155–175 (2002).
48. Bentley, K., Gerhardt, H. & Bates, P. A. Agent-based simulations of notch-mediated tip selection in angiogenic sprout initiation. *J. Theor. Biol.* **250**, 25–36 (2008).
49. Alarcón, T. & Page, K. M. Mathematical models of the VEGF receptor and its role in cancer therapy. *J. Roy. Soc. Interface* **4**, 283–304 (2007).
50. Stefanini, M. O., Wu, F. T., Mac Gabhann, F. & Popel, A. S. A compartment model of VEGF distribution in blood, healthy and diseased tissues. *BMC Syst. Biol.* **2**, 77 (2008).
51. Wu, F. T., Stefanini, M. O., Mac Gabhann, F. & Popel, A. S. A compartment model of VEGF distribution in human in the presence of soluble VEGF receptor-1 acting as a ligand trap. *PLoS ONE* **4**, e5108 (2009).
52. Folkman, J. Role of angiogenesis in tumor growth and metastasis. *Semin. Oncol.* **29**, S15–S18 (2002).
53. Jain, R. K. Determinants of tumor blood flow: a review. *Cancer Res.* **48**, 2641–2658 (1988).
54. Hahnfeldt, P., Panigrahy, D., Folkman, J. & Hlatky, L. Tumour development under angiogenic signalling: a dynamical theory of tumour growth, treatment response and postvascular dormancy. *Cancer Res.* **59**, 4770–4775 (1999).
55. Stoll, B. R., Migliorini, C., Kadambi, A., Munn, L. L. & Jain, R. K. A mathematical model of the contribution of endothelial progenitor cells to angiogenesis in tumors: implications for antiangiogenic therapy. *Blood* **102**, 2555–2561 (2003).
56. Stamper, I. J., Byrne, H. M., Owen, M. R. & Maini, P. K. Modelling the role of angiogenesis and vasculogenesis in solid tumour growth. *Bull. Math. Biol.* **69**, 2737–2772 (2007).
57. Arakelyan, L., Merbl, Y. & Agur, Z. Vessel maturation effects on tumour growth: validation of a computer model in implanted human ovarian carcinoma spheroids. *Eur. J. Cancer* **41**, 159–167 (2005).
58. Patel, A. A., Gawlinsky, E. T., Lemieux, S. K., Gatenby, R. A. Cellular automaton model of early tumour growth and invasion: the effects of native tissue vascularity and increased anaerobic tumour metabolism. *J. Theor. Biol.* **213**, 315–331 (2001).
59. Alarcón, T., Byrne, H. M. & Maini, P. K. A multiple scale model for tumour growth. *Multiscale Model Simul.* **3**, 440–475 (2005).
60. Gevertz, J. L. & Torquato, S. Modelling the effects of vasculature evolution on early brain tumour growth. *J. Theor. Biol.* **243**, 517–531 (2006).
61. Bauer, A. L., Jackson, T. L. & Jiang, Y. A cell-based model exhibiting branching and anastomosis during tumour-induced angiogenesis. *Biophys. J.* **92**, 3105–3121 (2007).
62. Owen, M. R., Alarcón, T., Maini, P. K. & Byrne, H. M. Angiogenesis and vascular remodelling in normal and cancerous tissues. *J. Math. Biol.* **58**, 689–721 (2009).
63. Macklin, P., McDougall, S., Anderson, A. R., Chaplain, M. A., Cristini, V. & Lowengrub J., Multiscale modelling and nonlinear simulation of vascular tumour growth. *J. Math. Biol.* **58**, 765–798 (2009).
64. Jain, R. K., Normalization of tumor vasculature: an emerging concept in antiangiogenic therapy. *Science* **307**, 58–62 (2005).
65. Deisboeck, T. S., Zhang, L., Yoon, J. & Costa, J. *In silico* cancer modelling: is it ready for prime time? *Nature Clin. Pract. Oncol.* **6**, 34–42 (2009).
66. Wheldon, T. E., Kirk, J. & Orr, J. S. Optimal radiotherapy of tumour cells following exponential-quadratic survival curves and exponential repopulation kinetics. *Brit. J. Radiol.* **50**, 681–682 (1977).
67. Wouters, B. G. & Brown, J. M. Cells at intermediate oxygen levels can be more important than the hypoxic fraction in determining tumour response to fractionated radiotherapy. *Radiat. Res.* **147**, 541–550 (1997).
68. McAnaney, H., O'Rourke, S. F. C. Investigation of various growth mechanisms of solid tumour growth within the linear quadratic model for radiotherapy. *Phys. Med. Biol.* **52**, 1039–1054 (2007).
69. Kirkpatrick, J. P. & Marks, L. B. Modelling killing and repopulation kinetics of subclinical cancer: direct calculations from clinical data. *Int. J. Radiat. Oncol. Biol. Phys.* **58**, 641–654 (2004).
70. Rockne, R., Alvord, E. C., Rockhill, J. K. & Swanson, K. R. A mathematical model for brain tumour response to radiation therapy. *J. Math. Biol.* **58**, 561–578 (2009).
71. Swanson, K. R., Bridge, C., Murray, J. D. & Alvord, E. C. Virtual and real brain tumours: using mathematical modelling to quantify glioma growth and invasion. *J. Neuro. Sci.* **216**, 1–10 (2003).
72. Szeto, M. D. *et al.* Quantitative metrics of net proliferation and invasion link biological aggressiveness assessed by MRI with hypoxia assessed by FMISO-PET in newly diagnosed glioblastomas. *Cancer Res.* **69**, 4502–4509 (2009).
73. Swanson, K. R., Alvord, E. C. & Murray, J. D. A quantitative model for differential motility of gliomas in grey and white matter. *Cell Prolif.* **33**, 317–329 (2000).
74. Whiteley, J. P. Gavaghan, D. J. Chapman, S. J. & Brady, J. M. Non-linear modelling of breast tissue. *Math. Med. Biol.* **24**, 327–345 (2007).
75. Araujo, R. P., Liotta, L. A. & Petricoin, E. F. Proteins, drug targets and the mechanisms they control: the simple truth about complex networks. *Nature Rev. Drug Discov.* **6**, 871–880 (2007).
76. Basse, B., Baguley, B. C., Marshall, E. S., Wake, G. & Wall, D. J., Modelling the flow [corrected] cytometric data obtained from unperturbed human tumour cell lines: parameter fitting and comparison. *Bull. Math. Biol.* **67**, 815–830 (2005).
77. Panetta, J. C. A mathematical model of breast and ovarian cancer treated with paclitaxel. *Math. Biosci.* **146**, 89–113 (1997).
78. Jain, R. K. & Baxter, L. T. Mechanisms of heterogeneous distribution of monoclonal antibodies and other macromolecules in tumors: significance of elevated interstitial pressure. *Cancer Res.* **48**, 7022–7032 (1988).
79. Byrne, H. M., Alarcón, T., Owen, M. R., Webb, S. W. & Maini, P. K. Modelling aspects of cancer dynamics: a review. *Philos. Transact. A Math. Phys. Eng. Sci.* **364**, 1563–1578 (2006).
80. Lowengrub, J. S. *et al.* Nonlinear modelling of cancer: bridging the gap between cells and tumour. *Nonlinearity* **23**, R1–R91 (2010).
81. Frieboes, H. B. *et al.* Prediction of drug response in breast cancer using integrative experimental/computational modelling. *Cancer Res.*, **69**, 4484–4492 (2009).
82. Jain, H. V., Nör, J. E. & Jackson, T. L. Quantification of endothelial cell-targeted anti-Bcl-2 therapy and its suppression of tumor growth and vascularization. *Mol. Cancer Ther.* **8**, 2926–2936 (2009).
83. Abdollahi, A. *et al.* Transcriptional network governing the angiogenic switch in human pancreatic cancer. *Proc. Natl Acad. Sci. USA.* **104**, 12890–12895 (2007).
84. Alarcón, T., Byrne, H. M. & Maini, P. K. Towards whole-body modelling of tumour growth. *Prog. Biophys. Mol. Biol.* **85**, 451–472 (2004).

**Acknowledgements**

H.M.B. would like to thank M. Owen (University of Nottingham, UK) for generating the multi-scale numerical simulations and also C. Lewis and G. Tozer (University of Sheffield, UK) for providing images from their laboratories. H.M.B. is also grateful to S. McElwain and D. Huttmacher (Queensland University of Technology, Australia) for their helpful and constructive comments on the Timeline.

**Competing interests statement**

The author declares no competing financial interests.

**DATABASES**

Entrez Gene: <http://www.ncbi.nlm.nih.gov/entrez/query.fcgi?db=gene>  
 APC | RB1 | TP53  
 UniProtKB: <http://www.uniprot.org>  
 ANGPT1 | ANGPT2 | VEGFA | VEGFR1 | VEGFR2

**FURTHER INFORMATION**

Helen M. Byrne's homepage:  
<http://www.maths.nottingham.ac.uk/personal/etzhmb/>

**SUPPLEMENTARY INFORMATION**

See online article: S1–4 (movies)

ALL LINKS ARE ACTIVE IN THE ONLINE PDF